Measurement of the Real-to-Imaginary Ratio of the $\bar{p}p$ Forward-Scattering Amplitudes

V. Ashford,[a] M. E. Sainio,[b] M. Sakitt, and J. Skelly
Brookhaven National Laboratory, Upton, New York 11973

and

R. Debbe, W. Fickinger, R. Marino, and D. K. Robinson
Case Western University, Cleveland, Ohio 44106
(Received 29 November 1984)

We have measured the ratio of the real to the imaginary parts of the $\bar{p}p$ forward-scattering amplitude in the incident-momentum range 360 to 650 MeV/c. These results are in good agreement with predictions of the Paris nucleon-antinucleon potential model which include spin-flip effects.

PACS numbers: 13.75.Cs

We report measurements of the ratio of the real to the imaginary parts of the $\bar{p}p$ forward-scattering amplitude, ρ, and compare the results to the predictions of the Paris $\bar{N}N$ potential model.[1] We demonstrate the importance of including the spin-flip amplitudes in the determination of ρ. Data were obtained at eleven values of the $\bar{p}p$ momentum between 360 and 650 MeV/c with a statistical precision of approximately ± 0.05.

The experiment was performed in the low-energy separated beam line (C4) at the Brookhaven National Laboratory alternating gradient synchrotron. With the exception of the hydrogen target, the experimental equipment, shown in Fig. 1, is the same as that which has been described in detail elsewhere.[2] The incoming antiproton was identified by time of flight, pulse height, and a Cherenkov threshold counter, which resulted in a tagged beam of greater than 99% purity. The beam trajectory was measured in four triplet drift chambers, each consisting of an x, u, and v plane. The 6-in.-long liquid-hydrogen target was designed to prevent bubbling. The scattered particle was measured in nine doublet drift chambers, three each for x, u, and v. The geometry was such that the transmitted beam passed normal to and through the center of all the chambers. Each of the two scintillator hodoscope arrays, $H1$ and $H2$, consisted of u and v coordinate slats. $H1$ had a square hole in the center to reduce the multiple scattering of the forward particles passing into the downstream drift chambers. The hodoscopes were used to monitor and meaure the drift-chamber efficiencies and to identify the scattered antiproton. The requirement that scattered antiprotons be identified by time-of-flight and pulse-height signals in both u and v hodoscope planes results in less than 5% contamination of the antiproton sample by misidentified pions. The resulting drift-chamber track reconstruction efficiency is about 97% in the forward direction.

We took data at each of the eleven momentum settings with both target full and target empty. Target-empty data were parametrized so that the target-empty subtractions could be made with data interpolated to the mometum values appropriate to the target-full data. In addition, a Monte Carlo technique was used to smear each event in the target-empty sample to match the calculated multiple scattering in the liquid-hydrogen target.

We show in Fig. 2 the eleven $\bar{p}p$ elastic differential cross sections. To extract the ratio of the real to the imaginary parts of the forward-elastic-scattering amplitude from these data, we initially adopt the standard formalism which neglects spin-flip amplitudes. The scattering cross section is a sum of three parts: a Coulomb, a nuclear, and a Coulomb-nuclear interfer-

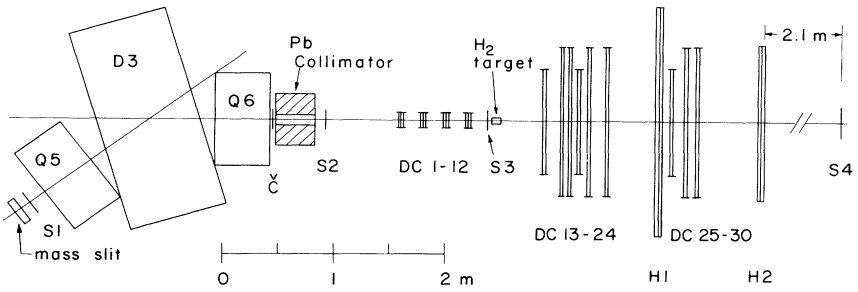

FIG. 1. Layout of the antiproton scattering experiment.

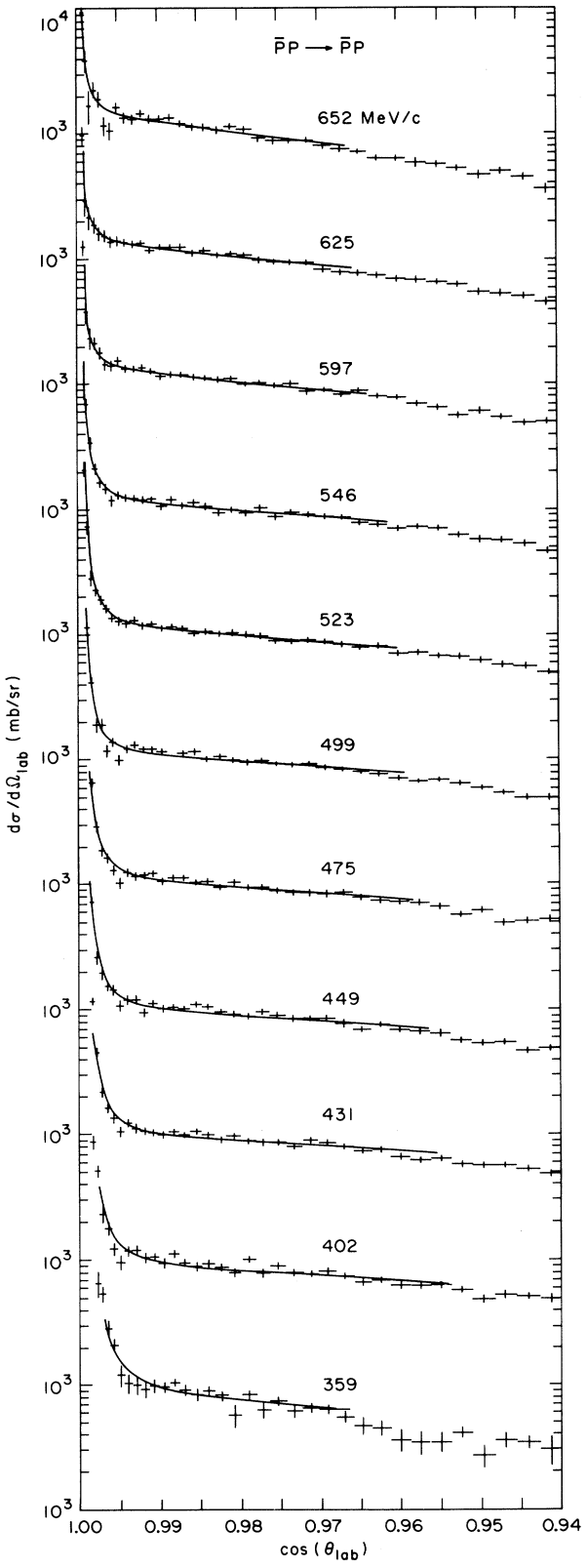

FIG. 2. Elastic differential cross section for different momenta. The curves represent fits described in the text.

ence term. Explicitly we have

$$\frac{d\sigma^C}{dt} = 4\pi\left(\frac{\alpha\hbar c}{\beta t}\right)^2 F(t)^2,$$

$$\frac{d\sigma^N}{dt} = \frac{1}{\pi}\left(\frac{\sigma_{tot}}{4\hbar c}\right)^2 (1+\rho^2)\exp(-bt),$$

and

$$\frac{d\sigma^I}{dt} = \frac{\alpha\sigma_{tot}}{\beta t} F(t)\exp(-\tfrac{1}{2}bt)(\rho\cos\delta - \sin\delta),$$

where $-t$ is the four-momentum transfer, α is the fine-structure constant, β is the laboratory velocity of the incident $\bar{p}$, b is the slope parameter of the $\bar{p}p$ diffraction peak, $F(t)$ is the Coulomb form factor of the proton, $F(t) = (1 + t/0.71)^{-4}$, σ_{tot} is the $\bar{p}p$ total cross section, and δ is the phase of the Coulomb amplitude, $\delta = -[\ln(R^2 t) + 0.5772]\alpha/\beta$, with $R^2 = 9.5$ GeV^{-2}. For the total cross section, we use the parametrization $\sigma_{tot} = (61.2\text{ mb}) + (53.4\text{ mb GeV}/c)/P$. This function is the result of a fit to published total cross-section data.[3]

The data have been fitted by a convolution of the scattering cross section with our experimental angular resolution. We fit for the two parameters ρ and b. We exclude from our fits the extreme forward points which are completely dominated by multiple scattering. The upper limit on the range of angles included in each fit varied linearly from 17° (laboratory angle) at 402 MeV/c to 14° at 695 MeV/c. This was necessary since at larger angles the data clearly depart from an exponential in bt. Such a departure from simple exponential behavior is expected from $\bar{N}N$ potential models. Furthermore, for the lowest momentum (360 MeV/c), it was necessary to reduce this upper limit to 14.5° to get a reasonable fit. The results of the fits and the angular ranges over which the fits were made are listed in Table I.

Plots of ρ and b versus momentum from the fits are shown as closed circles in Fig. 3. The statistical errors presented in Fig. 3 and Table I are the diagonal elements of the error matrix. A typical χ^2 contour plot for ρ and b, illustrating the correlations between these variables, is shown in Fig. 4. The values of ρ and b are subject to systematic uncertainties including those in beam momentum and in the density of the liquid hydrogen. We estimate that each of these uncertainties is less than 2% and that they affect the fitted parameters in the following way. A shift of $\pm 2\%$ in the beam momentum produces a shift of roughly $\mp 1.3\%$ in σ_{tot} which in turn results in a uniform change of ± 0.03 in ρ and ∓ 1.0 (GeV/c)$^{-2}$ in b. On the other hand, a shift of $\pm 2\%$ in our overall normalization systematically changes the values of ρ by about ± 0.03 and those of b by about ∓ 1.0 (GeV/c)$^{-2}$. These shifts are comparable to the statistical errors.

TABLE I. Results of fits to the forward-scattering differential cross sections.

P (MeV/c)	$\theta_{c.m.}$ range (degrees)	$\eta=0$ ρ	$\eta=0$ b [(GeV/c)$^{-2}$]	$\eta=\eta(P)$ ρ	$\eta=\eta(P)$ b [(GeV/c)$^{-2}$]
652	4.5–14.5	0.197 ± 0.026	21.73 ± 0.85	0.087 ± 0.040	23.36 ± 0.85
625	4.0–17.0	0.083 ± 0.034	18.23 ± 0.80	−0.061 ± 0.074	21.57 ± 0.80
597	3.5–16.7	0.119 ± 0.026	18.79 ± 0.80	−0.001 ± 0.047	21.83 ± 0.80
546	3.0–16.5	0.061 ± 0.027	19.12 ± 0.83	−0.044 ± 0.042	23.61 ± 0.80
523	3.0–16.3	0.090 ± 0.023	20.01 ± 0.82	−0.016 ± 0.037	24.23 ± 0.83
499	2.5–16.0	0.046 ± 0.028	18.98 ± 0.90	−0.083 ± 0.050	24.33 ± 0.90
475	2.5–15.8	0.097 ± 0.023	22.52 ± 1.05	−0.005 ± 0.034	27.41 ± 1.05
449	2.5–15.5	0.015 ± 0.029	23.38 ± 1.15	−0.100 ± 0.043	30.36 ± 1.15
431	2.0–15.0	0.030 ± 0.027	22.63 ± 1.30	−0.073 ± 0.039	29.90 ± 1.30
402	2.0–14.7	−0.024 ± 0.037	27.40 ± 1.70	−0.156 ± 0.058	36.57 ± 1.68
359	2.0–14.4	0.023 ± 0.042	44.15 ± 5.55	−0.047 ± 0.052	56.78 ± 5.50

Our results are consistent with small values of ρ, between 0.0 and 0.2, with no significant structure throughout this momentum region. These results show less momentum dependence than those reported by Iwasaki *et al.*,[4] but are in agreement with the results of reanalysis in terms of the standard formalism of the same data.[3]

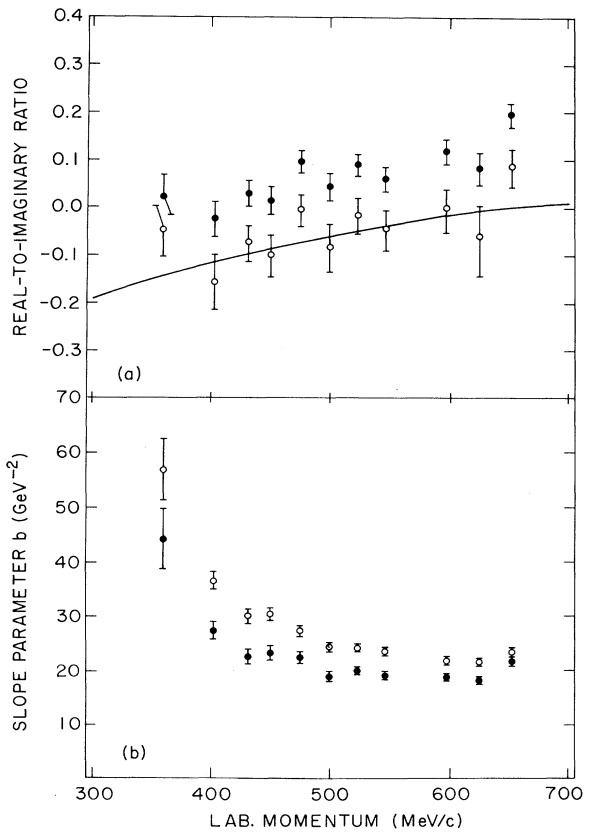

FIG. 3. Results for (a) the ratio of the real to the imaginary parts of the forward-scattering amplitude and (b) the slope parameter as a function of incident $\bar{p}$ momentum. The two sets of data and the solid curve are described in the text.

Current theoretical models for NN and $\bar{N}N$ scattering include contributions from spin-flip amplitudes which have been ignored in the preceding analysis. We have therefore made a second set of fits which include contributions from the spin-flip amplitudes and compare the results with predictions of the Paris $\bar{N}N$ model. This model uses the G parity transformed NN Paris potential[5] for the real part and parametrizes the annihilation as a purely imaginary part in order to fit published $\bar{p}p$ elastic and total cross sections. The result is a potential having strong spin, isospin, and energy dependence.

If we assume that both the spin-flip and the non-spin-flip amplitudes have the same t dependence, then the nuclear scattering term is multiplied by a factor

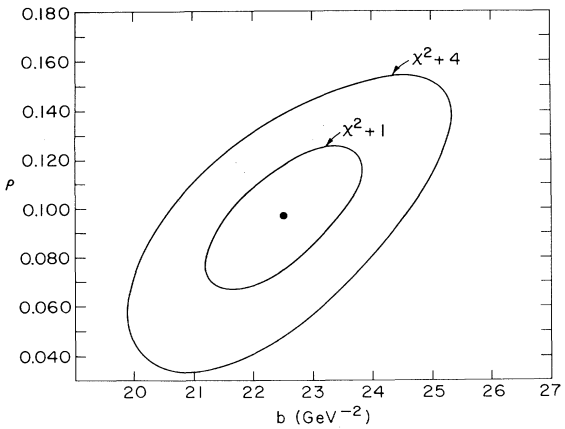

FIG. 4. χ^2 contours for a typical fit to ρ and b.

$(1+\eta^2)$, where η is the ratio of the spin-flip to non-spin-flip parts of the forward amplitude.[1] Since there are strong correlations among ρ, b, and η, we have made fits for ρ and b, fixing the values of η to those predicted by the Paris model.[1,6] We parametrized the predicted values of η as $\eta(P)=0.3698-(0.1384\times P)$ and used this function in our analysis. We have parametrized the prediction of ρ as

$$\rho(P)=-0.5004+(1.2658\times P)-(0.7678)P^2$$

and plot it for comparison in Fig. 3(a). P is the incident momentum in GeV/c. The resulting values of ρ and b are shown in the right-hand columns in Table I and by open circles in Figs. 3(a) and 3(b). The ρ values are systematically shifted downward an average of 0.11 from those for $\eta=0$. The accumulated χ^2/d.o.f. for the eleven fits with $\eta=0$ was 1.39; the fits with the spin-flip term was somewhat better with an accumulated χ^2/d.o.f. of 1.16 and had somewhat weaker correlation between ρ and b.

In summary, our results are in good agreement with a self-consistent set of ρ and η parameters as predicted by the Paris $\bar{N}N$ model which supports the existence of bound states. The fitted values listed in the right half of Table I are our best estiamtes of ρ in this momentum range.

We thank the Alternating Gradient Synchrotron Department of Brookhaven National Laboratory. This work was supported by the U. S. Departmnt of Energy under Contract No. DE-AC02-76-CH00016 and by the National Science Foundation under Contract No. PHY 80-20418.

[a]Present address: Stanford Linear Accelerator Center, Stanford, Cal. 94305.

[b]Present address: Schweizerisches Institut für Nuklearforschung, CH-5234 Villigen, Switzerland.

[1]M. Lacombe, B. Loiseau, B. Moussallam, and R. Vinh Mau, Phys. Lett. **124B**, 443 (1983).

[2]V. Ashford *et al.*, Phys. Rev. C **30**, 1080 (1984).

[3]K. Nakamura *et al.*, Phys. Rev. D **29**, 349 (1984).

[4]H. Iwasaki *et al.*, Phys. Lett. **103B**, 247 (1981).

[5]M. Lacombe *et al.*, Phys. Rev. C **21**, 861 (1980).

[6]J. Côté, M. Lacombe, B. Loiseau, B. Moussallam, and R. Vinh Mau, Phys. Rev. Lett. **48**, 1319 (1982).